Journal of Biomechanics 48 (2015) 3701–3708

Contents lists available at ScienceDirect

Journal of Biomechanics

journal homepage: www.elsevier.com/locate/jbiomech
www.JBiomech.com

Exploring interactions between force, repetition and posture on intervertebral disc height loss and bulging in isolated porcine cervical functional spinal units from sub-acute-failure magnitudes of cyclic compressive loading

Chad E. Gooyers [1], Jack P. Callaghan *

Department of Kinesiology, Faculty of Applied Health Sciences, University of Waterloo, Waterloo, Ontario, Canada N2L 3G1

ARTICLE INFO

Article history:
Accepted 18 August 2015

Keywords:
Intervertebral disc
Annulus fibrosus
Height loss
Bulging
Laser scanner

ABSTRACT

Most *in vitro* studies are limited in the ability to partition intervertebral disc (IVD) height loss from total specimen height loss since the net changes in the actuator position of the materials testing system simply reflect net changes to functional spinal units (FSUs) used for testing. Three levels of peak compressive force, three cycle rates and two dynamic postural conditions were examined using a full-factorial design. Cyclic compressive force was applied using a time-varying waveform with synchronous flexion/extension for 5000 cycles. Surface scans from the anterior aspect of the IVD were recorded in a neutral and flexed posture before and after the cyclic loading protocol using a 3D laser scanner to characterise changes in IVD height loss and bulging. A significant three-way interaction ($p=0.0092$) between the magnitude of peak compressive force, cycle rate and degree of postural deviation was observed in cycle-varying specimen height loss data. A significant main effect of peak compressive force ($p=0.0003$) was also observed in IVD height loss calculated from the surface profiles of the IVD. The relative contribution of IVD height loss (measured on the anterior surface) to total specimen height loss across experimental conditions varied considerably, ranging from 19% to 58%. Postural deviation was the only factor that significantly affected the magnitude of peak AF bulge ($p=0.0016$). This investigation provides evidence that total specimen height loss is not an accurate depiction of cycle-varying changes in the IVD across a range of *in vivo* scenarios that were replicated with *in vitro* testing.

1. Introduction

Specimen height loss is a dependent measure that is commonly examined in spine biomechanics *in vitro* studies. Previous research conducted by van der Veen et al. (2008) has demonstrated that deformation in the intervertebral disc (IVD), cartilaginous endplates and vertebrae all contribute to the total height loss of a functional spinal unit (FSU) mechanically loaded in compression. Unfortunately, most studies are limited in the ability to partition this height loss across each of these anatomical structures since the net differences in the actuator position of the materials testing system simply reflect overall changes to the entire osteoligamentous system of FSUs and mounting interfaces used for testing. Of clinical importance, exaggerated height loss has been linked to IVD bulging, which is a known mechanism for low back pain due to compression of the spinal cord in the spinal canal or impingement of the nerve roots in the neural foramina (Brinckmann et al., 1989; Cuchanski et al., 2011; Stokes, 1988; Wenger and Schlegel, 1997).

Therefore, the primary objective of this study was to explore interactions between: (i) the magnitude of the applied compressive force, (ii) cycle rate and (iii) degree of postural deviation on IVD height loss in isolated porcine cervical FSUs subjected to sub-maximal cyclic compressive loading. A secondary objective was to quantify the amount of pre/post-annulus fibrosus (AF) bulging across loading conditions to better understand the structural changes that occur in the IVD of intact FSUs under cyclic loading conditions.

2. Materials and methods

2.1. Specimen preparation

The cervical spines of 63 porcine specimens (mean age=6 months, weight=85 kg) were obtained following death and stored frozen at −20 °C. The cervical spine was separated into two FSUs for testing, which included two adjacent vertebral bodies and

* Corresponding author: Tel.: +1 519 888 4567x37080;fax: +1 519 746 6776.
E-mail address: callagha@uwaterloo.ca (J.P. Callaghan).
[1] Present address: Giffin Koerth Forensic Engineering & Science, 40 University Avenue, Toronto, Ontario, Canada M5J 1T1.

http://dx.doi.org/10.1016/j.jbiomech.2015.08.023
0021-9290/

the IVD at the level of c34 and c56; resulting in a total of 126 FSUs that were initially included in the study. Porcine cervical FSUs were used as surrogates for the human lumbar spine due to their anatomical and functional similarities (Oxland et al., 1991; Yingling et al., 1999), providing superior control over potential confounding factors that can impact the mechanical integrity of the tissues surrounding the intervertebral joint (e.g. age, diet, physical activity). The inclusion criteria for specimens included in this investigation required that FSUs met a non-degenerated disc quality (Grade 1) as outlined by Galante (1967). Before testing, frozen specimens were thawed at room temperature for a minimum of 12 h. Dissection of the cervical spine involved isolating the two FSUs of interest and carefully removing the surrounding musculature, leaving only the osteoligamentous structures intact, except for the portion of the anterior longitudinal ligament that attached directly to the anterior surface of the AF, which was removed to expose the IVD for surface profile scanning. Once the dissection protocol was complete, width and depth measurements of the two exposed endplates were recorded using digital calipers. These measurements were used to estimate an average intervertebral joint endplate surface area using the equation of an ellipse that were used as input for a regression equation, which was developed using porcine cervical FSUs, to approximate each specimen's ultimate compressive tolerance (UCT) without destructive testing (Parkinson et al., 2005). This allowed for normalisation of peak compressive loading across specimens. Next, the locations of the cartilaginous endplates on the anterior surface of the FSU were marked with three steel pins (0.5 mm diameter; 6 per specimen). One pin was placed at the centre of the IVD and two on the anterolateral sides (Fig. 1). This was done to facilitate pre/post-registration and alignment of the resultant 3D surface profiles obtained from the anterior surface of the IVD from each FSU. The superior and inferior vertebrae of the FSU were then fixed within custom-machined aluminium cups using a combination of wood screws (fixed 1 cm into the exposed endplates) and non-exothermic dental plaster (Denstone; Miles, Southbend, IN, USA). To prevent specimen dehydration throughout the dissection and potting procedures, all FSUs were kept hydrated with a saline mist (0.9% weight per volume [w/v] solution) that was applied approximately every 15 min.

2.2. Procedure

Potted specimens were mounted in a servo-hydraulic materials testing system (Model 8872; Instron, Canton, MA, USA), modified to apply flexion/extension motion to the FSU while under compressive load. Each specimen was free to translate in the anterior–posterior direction (via bearing tray), which enabled the centre of rotation to translate within the joint during the cyclic loading protocol. To minimise dehydration during the prolonged mechanical exposure, all specimens were wrapped in saline soak gauze (0.9% w/v solution) and plastic wrap. Each FSU initially received 15 min of static compressive force (300 N) to counter any post-

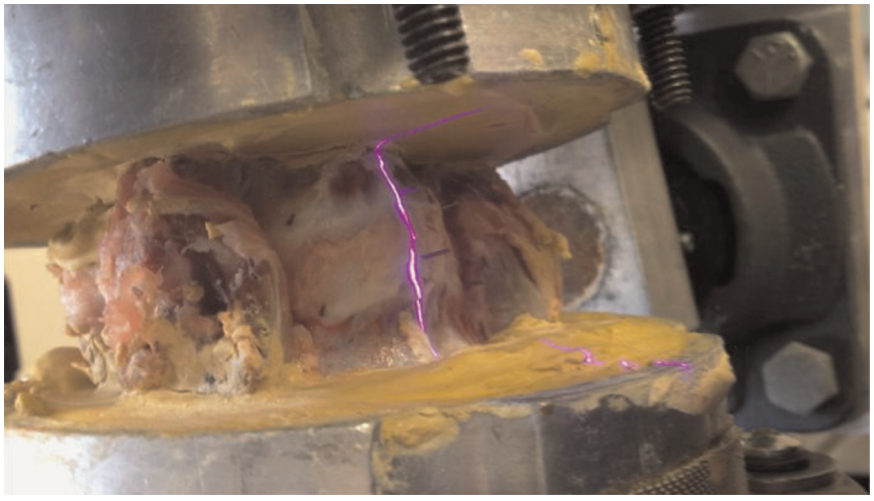

Fig. 1. Functional spinal unit potted in custom machined aluminium cups with non-exothermic dental plaster (yellow) and mounted in a modified materials testing system. Three stainless steel pins (0.5 mm diameter) were inserted into the superior and inferior cartilaginous endplates (6 total) to facilitate pre/post-registration of the 3D surface profile and identify the superior and inferior boundaries of the IVD. The visible (blue) laser on the anterior surface of the FSU was translated across the specimen to construct individual surface profiles. The test specimen is shown with the plastic backed saline infused gauze material removed that was in place during testing to prevent dehydration of test samples. (For interpretation of the references to colour in this figure legend, the reader is referred to the web version of this article.)

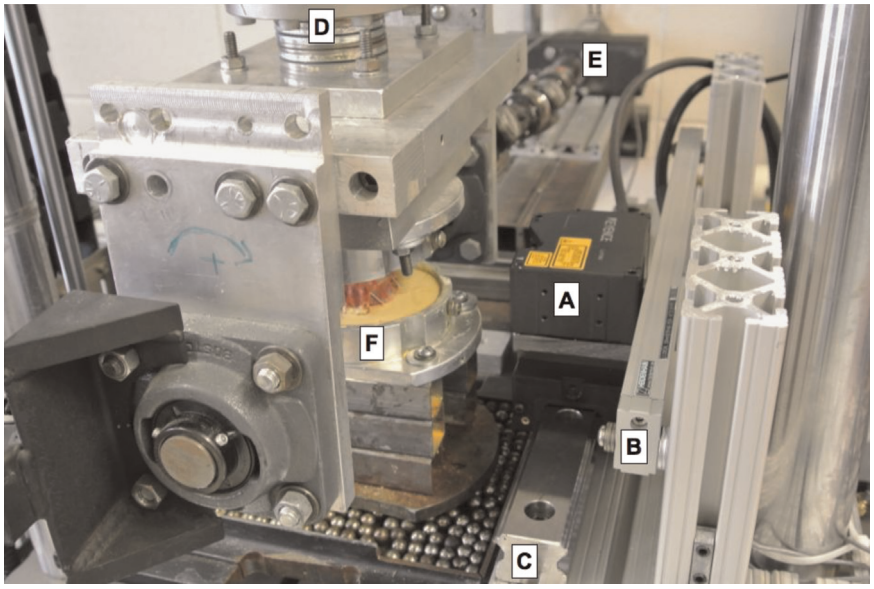

Fig. 2. Modified materials testing apparatus with 3D laser scanning system that was employed for testing. (A) 2D laser head, (B) linear encoder, (C) linear guide, (D) 20 kN load cell in-line with Instron actuator, (E) flexion/extension torque motor, and (F) functional spinal unit potted in custom machined aluminium cups with non-exothermic dental plaster.

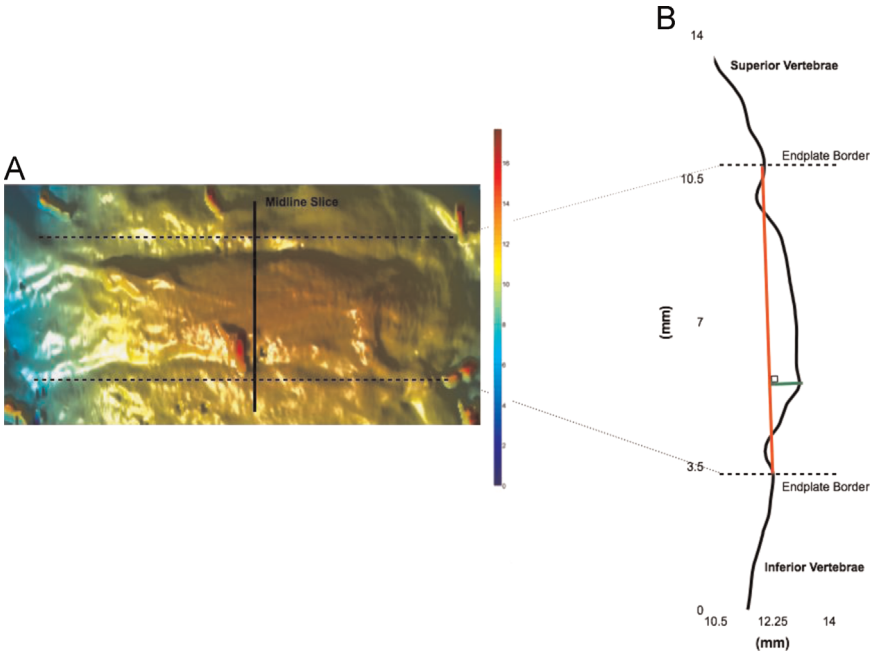

Fig. 3. (A) Resultant 3D profile of the anterior surface of the intervertebral disc and (B) convention used to report bulging measurements (mm) of the annulus fibrosus in a flexed posture. The magnitude of the annulus fibrosus bulge is shown as the green vector, perpendicular to the vector defined by the endpoints of the superior and inferior endplates. (For interpretation of the references to colour in this figure legend, the reader is referred to the web version of this article.)

mortem swelling (mean height loss = 0.95 mm; SD = 0.20) that occurred within the specimen. During this preload test, an independent servomotor (AKM23D; Kollmorgen/Danaher Motion, Radford, VA, USA) connected in-series with a torque cell (T120-106-1K; SensorData Technologies Inc., Sterling heights, MI, USA) was used to establish the angular position of minimal passive stiffness about the flexion/extension axis. Following the preload test, three cycles of passive flexion–extension (PFE) joint rotations were applied (rate = 0.5° per second) to identify the limits of each FSU's neutral zone in the sagittal plane. Using custom software, interfaced with an ISA bus motion controller (Model DMC18 × 0, Galil Motion Control, Rocklin, CA USA), the applied moment and angular displacement were continuously sampled at 25 Hz. The flexion and extension limits of the neutral zone were identified using methods described by Thompson et al. (2003), which were used to define the dynamic flexion/extension postures that were applied during testing.

Upon completion of both the preload and PFE tests, specimens were randomly assigned to 1 of 18 experimental conditions. Three levels of peak compressive force (10%, 20% and 40% of specimens' UCT), three cycle rates (5, 10 and 30 cycles per minute), and two dynamic postural conditions, including: (i) 100% neutral zone range; average (SD) of 6.79° (2.23) and (ii) 300% neutral zone range; 20.52° (4.41) were examined using a full-factorial design. Compressive force was applied using a time-varying waveform (two-seconds duration) based on estimates of *in vivo* loading using a dynamic EMG-assisted model of the lumbar spine (Parkinson and Callaghan, 2009). The applied compressive force was scaled to the desired peak load. Dynamic flexion/extension was synchronously applied to FSUs during each loading cycle using a motion profile recorded from the lumbar spine during the same floor to waist height lift (Parkinson and Callaghan, 2009), and was scaled for each posture condition to 100% and 300% of the specimens' neutral zone range. Specimens were positioned in a neutral posture between loading cycles.

All FSUs were cyclically loaded for 5000 cycles or until fatigue failure occurred, which was identified by specimen height loss greater than 9 mm (Parkinson and Callaghan, 2009). Throughout testing, measurements of the applied compressive force and vertical position of the Instron actuator were continuously sampled at 32 Hz using a 16-bit analog-to-digital conversion board (National Instruments, Austin, TX, USA). In addition, a high-speed, 2D laser displacement sensor (LJ-V7080, Keyence Corporation, Osaka, Japan) was used to characterise the anterior surface profile of the IVD. The 2D laser displacement sensor (Fig. 2) was mounted on a 48 cm linear guide (NSK Ltd., Tokyo, Japan) and interfaced with a glass scale incremental encoder (LS 328-C, Heidenhain, Schaumburg, IL, USA; accuracy 10 μm) to obtain a 3D cross-sectional scan of the anterior surface of the FSU every 40 μm in the frontal plane. The manufacturer's specifications indicated that the laser displacement sensor had an accuracy of 46 μm in the transverse direction (i.e. primary bulge axis) and resolution of 20 μm in the vertical direction (i.e. primary IVD height loss axis). Surface scans were recorded in both a neutral and flexed posture, which were recorded in less than two-seconds.

2.3. Data processing

All mechanical waveforms were processed in MATLAB (version R2013b, Mathworks, Natick, MA). Each signal was dual-pass filtered with a 2nd order low-pass digital Butterworth filter, with an effective cutoff frequency of 10 Hz. Individual loading cycles were identified using the compressive force waveform. Laser scanner data were processed in MATLAB (version R2013b, Mathworks, Natick, MA). Each 2D scan captured every 40 μm along the anterior surface of the FSU (i.e., a total of M scans in the frontal plane) was "stitched together" to create an M × 800 data matrix, which was digitally filtered using a 2D median spatial filter to reduce noise and preserve edges. Sufficient data was captured surrounding the perimeter of the IVD to ensure that any distortion introduced by the median filter did not affect the resultant 3D surface profile of the IVD.

2.4. Dependent measures

Peak specimen height loss as measured by the axial position of the Instron actuator was calculated after 1, 10, 100, 1000, 2000 and 5000 cycles in the neutral posture. Intervertebral disc height loss calculated as the vertical distance between the superior and inferior endplates was computed from pre/post-3D anterior surface profiles that were rendered for each specimen in a neutral posture. Similarly, the peak disc bulge, calculated from the anterior surface of the IVD, was computed at the midline from the 3D surface profiles captured in a flexed posture, pre/post-testing. To facilitate the comparison of AF bulge measurements between specimens and improve the anatomical interpretation of this measure, the maximum bulge perpendicular to a vector defined by the endpoints of the superior and inferior endplates has been reported (Fig. 3).

2.5. Statistical analyses

Due to technical difficulties in synchronising the cyclic compressive load with the flexion/extension axes, three FSUs were excluded; resulting in a total of 123 specimens that were considered for the study. Specimens from the 5 cycles per minute, 100% neutral zone range, 40% UCT loading condition were also excluded since there were no specimens that survived the entire cyclic loading protocol. All statistical analyses were computed using SAS software (version 9.2, SAS Institute Inc., Cary, NC) with a significance level (α) of 0.05 determined *a priori*. To examine interactions between the magnitude of peak compressive force, cycle rate and degree of postural deviation on cycle-varying specimen height loss, a four-factor mixed general linear model was applied, with cycle number as a repeated measure. Simple effects were used to analyse all significant interactions. Effect sizes for all significant comparisons were evaluated using Cohen's *d*, using a pooled estimate of the population standard deviation from both groups (Cohen, 1988).

3. Results

3.1. Specimen randomisation

Successful randomisation and consistency of FSUs across experimental conditions were achieved, as there were no significant main effects of force, cycle rate or postural deviation revealed in estimates of endplate area ($p=0.7197$, 0.7316 and 0.4382, respectively) or neutral zone range, as determined by the passive flexion–extension tests ($p=0.7812$, 0.5998 and 0.6010, respectively).

3.2. Specimen height loss

A significant three-way interaction ($p=0.0092$) between the magnitude of peak compressive force, cycle rate and degree of postural deviation was observed in cycle-varying specimen height loss data (Fig. 4), as calculated using the axial position of the Instron actuator. Subsequent analysis of the interaction between cycle rate and postural deviation at each magnitude of compressive load revealed that significant main effects of cycle number ($p<0.0001$), cycle rate ($p<0.0001$) and postural deviation ($p<0.0001$) emerged in specimens assigned to the 10% UCT group. Specifically, FSUs assigned to the 10% UCT group that were cyclically loaded at a rate of 10 cycles per minute experienced significantly greater height loss compared to the 5 cycles ($p<0.001$; $d=0.37$; mean difference=0.22 mm) and 30 cycles per minute conditions ($p=0.0020$; $d=0.12$; mean difference=0.07 mm). Moreover, specimens in the 10% UCT group that were cyclically loaded at 30 cycles per minute experienced significantly greater height loss compared to those in the 5 cycles per minute conditions ($p=0.0057$; $d=0.24$; mean difference=0.14 mm). There was no significant difference ($p>0.4420$) in the magnitude of specimen height loss in the first 100 loading cycles; however, significant differences ($p<0.0020$; $d>0.71$) were noted in all comparisons after 1000 cycles. When considering the effect of postural deviation at 10% UCT, specimens that were flexed/extended to 300% of their neutral zone range experienced significantly greater height loss ($p<0.0001$, $d=0.47$; average difference=0.28 mm) compared to the 100% condition.

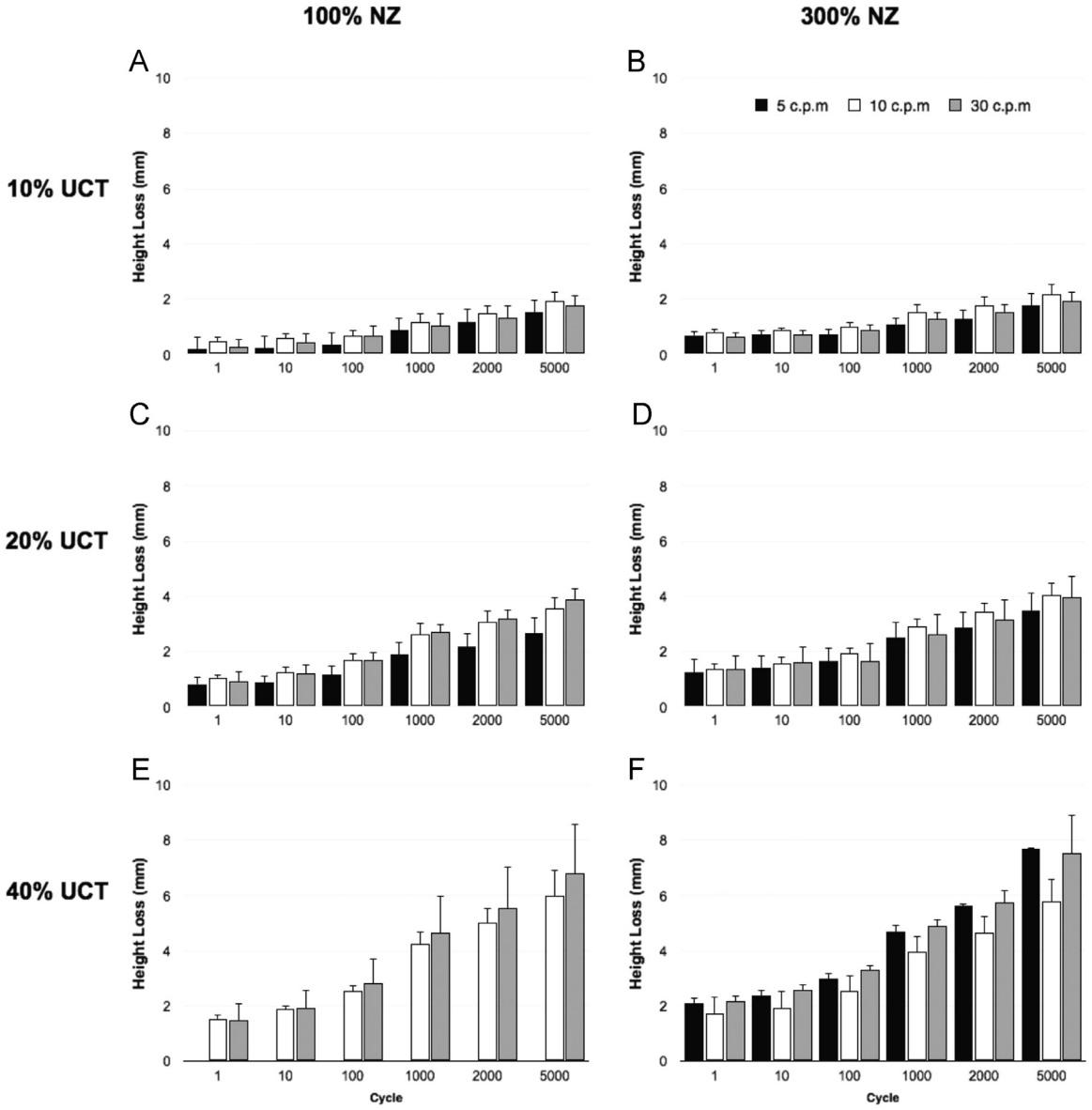

Fig. 4. Cycle-varying specimen height loss across: (A) 10% ultimate compressive tolerance (UCT)@100% neutral zone (NZ); (B) 10% UCT@300% NZ; (C) 20% UCT@100% NZ; (D) 20% UCT@300% NZ; (E) 40% UCT@100% NZ; (F) 40% UCT@300% NZ. Specimens from the 5 cycles per minute, 100% neutral zone range, 40% UCT loading condition were excluded since there were no specimens that survived the entire loading protocol.

A significant two-way interaction ($p=0.0054$) between cycle rate and postural deviation was observed in specimens that were cyclically loaded at 20% UCT. There was no significant difference ($p=0.7876$) in the magnitude of height loss that was observed between the 100% and 300% neutral zone range postural deviations at a rate of 30 cycles per minute; despite the significant increase that was observed in the 300% neutral zone range condition at a rate of 5 ($p<0.0001$, $d=0.66$; mean difference=0.60 mm) and 10 ($p=0.0211$, $d=0.34$; mean difference=0.34 mm) cycles per minute. A significant main effect of cycle number ($p<0.0001$) was also noted; however, there were no significant differences in the magnitude of height loss in the first 10 loading cycles ($p=0.3784$). All other comparisons at 100, 1000, 2000 and 5000 cycles were significantly different ($p<0.0330$, $d>0.70$), with greater height loss measured with increasing loading cycles.

Significant main effects of cycle rate ($p=0.0082$) and cycle number ($p<0.001$) were noted in specimens that were cyclically loaded at 40% UCT. Tukey's *post-hoc* test revealed that specimens assigned to both the 5 and 30 cycles per minute conditions experienced significantly greater height loss ($p<0.05$, $d>0.27$) compared to the 10 cycles per minute condition. No difference was observed between the 5 and 30 cycles per minute conditions. There were no significant differences in the magnitude of height loss in the first 10 loading cycles; however, all other comparisons at 100, 1000, 2000 and 5000 cycles were significantly different ($p<0.05$, $d>0.88$), with greater height loss occurring with increasingly more loading cycles.

3.3. Intervertebral disc height loss

A significant main effect of peak compressive force magnitude ($p=0.0003$) was observed in IVD height loss data, as calculated from the 3D surface profiles of each FSU captured in a neutral posture, pre/post-testing. Main effects of cycle rate and degree of postural deviation were not significant ($p=0.54$ and 0.95, respectively). Overall, a peak compressive force of 40% UCT was associated with significantly greater IVD height loss compared to the 10% ($p<0.05$, $d=1.38$) and 20% ($p<0.05$, $d=1.11$) loading conditions. A summary of IVD height loss across experimental conditions is provided in Fig. 5. The average relative contribution of IVD height loss (measured on the anterior surface of the IVD) to total specimen height loss varied across experimental conditions, ranging from 19% to 58% (Table 1). Scatter plots illustrating linear regression analyses between IVD height loss and specimen height loss across all experimental conditions for the 10% and 20% UCT force conditions are provided in Fig. 6. Overall, total specimen height loss was a poor description of IVD height loss. A wide range of Pearson product–moment correlations were observed (−0.54 to 0.95) across experimental conditions.

3.4. Intervertebral disc bulging

Significant main effects of postural deviation ($p=0.0016$) and time ($p=0.0423$) were observed in peak AF bulge measurements. *Post-hoc* analyses revealed that specimens exposed to repetitive postural deviation of 100% NZ range exhibited significantly greater anterior bulge ($p<0.05$, $d=0.42$, mean difference=0.23 mm) compared to those assigned to the 300% condition. Moreover, the anterior bulging of the AF in a flexed posture was found to be significantly greater ($p<0.05$, $d=0.03$, mean difference=0.17 mm) in 3D scans captured prior to the cyclic mechanical exposure. A summary of the average AF bulge measurements recorded at the midline of the IVD across experimental conditions is provided in Fig. 7. Scatter plots illustrating linear regression analyses between

Table 1
Average relative contribution of intervertebral disc height loss compared to total specimen height loss.

Force (% UCT)	Repetition (cycles per minute)	Posture (% NZ)	Average relative contribution[a]	Standard deviation
10	5	100	0.49	0.34
10	5	300	0.19	0.10
10	10	100	0.38	0.15
10	10	300	0.27	0.18
10	30	100	0.58	0.14
10	30	300	0.49	0.21
20	5	100	0.34	0.18
20	5	300	0.35	0.30
20	10	100	0.33	0.22
20	10	300	0.26	0.16
20	30	100	0.26	0.13
20	30	300	0.21	0.14
40	5	100	–	–
40	5	300	0.15	0.13
40	10	100	0.26	0.05
40	10	300	0.18	0.06
40	30	100	0.21	0.11
40	30	300	0.20	0.08

[a] Relative contribution=IVD height loss (mm)/specimen height loss (mm)
*specimens from the 5 cycles per minute, 100% neutral zone range, 40% UCT loading condition were excluded since there were no specimens that survived the entire loading protocol.

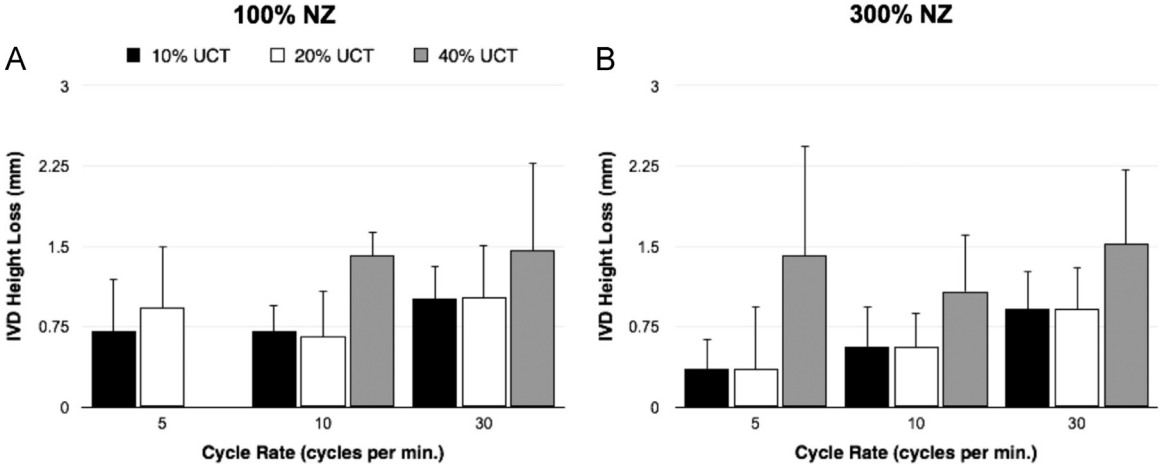

Fig. 5. Intervertebral height loss as calculated from the 3D surface profile of the anterior aspect of the IVD, separated by (A) 100% and (B) 300% neutral zone postural deviation. Specimens from the 5 cycles per minute, 100% neutral zone range, 40% UCT loading condition were excluded since there were no specimens that survived the entire loading protocol.

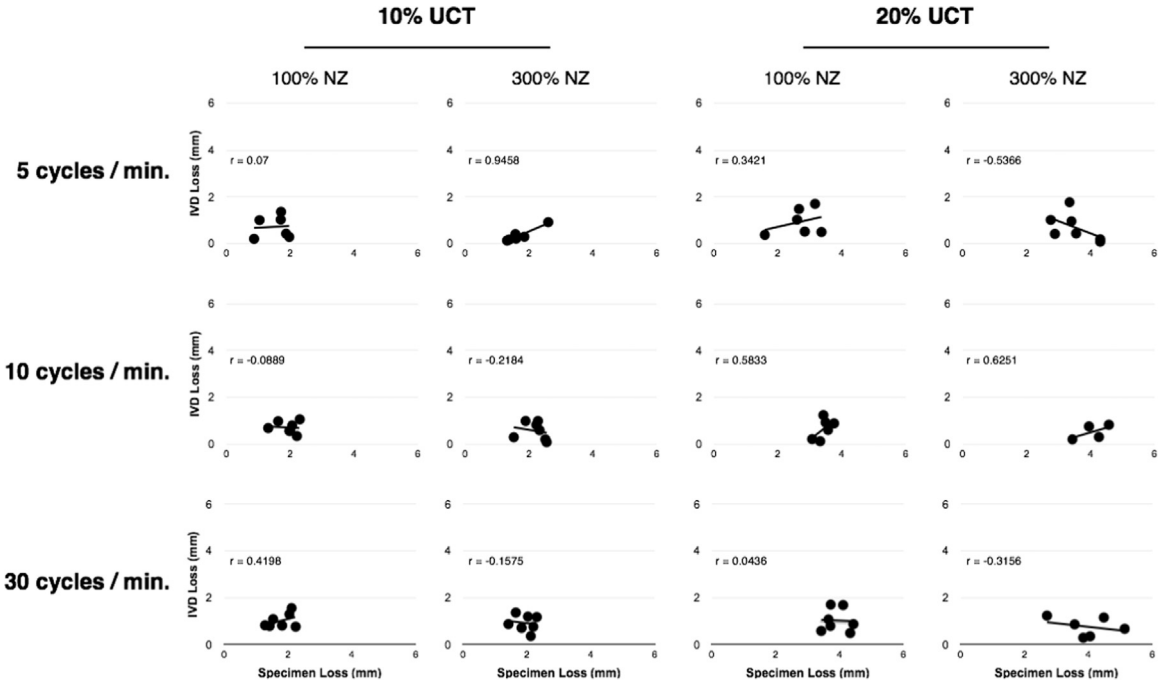

Fig. 6. Scatter plots illustrating linear regression analyses that were performed between intervertebral height loss and specimen height loss data across experimental conditions in both the 10% and 20% ultimate compressive tolerance loading conditions.

IVD height loss and IVD bulging across all experimental conditions for the 10% and 20% UCT force conditions are provided in Fig. 8. Overall, a wide range of Pearson product–moment correlations were observed (–0.44 to 0.78) between IVD height loss and IVD bulging across experimental conditions.

4. Discussion

Consistent with our hypothesis, a significant three-way interaction emerged in cycle-varying measures of specimen height loss; however, it is interesting that the magnitude of the applied load was the only exposure found to significantly impact IVD height loss (measured on the anterior surface of the IVD). This suggests that the interaction observed in specimen height loss may have been driven by time-varying changes in either the cartilaginous endplates or the vertebral bodies.

The relative contribution of IVD height loss to total specimen height loss was shown to vary across experimental conditions (ranging from 19% to 58%) with the greatest relative proportion observed in the 10% UCT loading group (average relative contribution = 40%), which is likely due to the reduced magnitude of total specimen height loss. Overall, total specimen height loss was a poor descriptor of pre/post-changes in the IVD. However, it must be acknowledged that only the anterior surface of the IVD was imaged, and that multiple load transmission pathways exist in a FSU. Therefore, it is possible that our results may not reflect structural changes in other regions of the IVD. Nonetheless, our hypothesis that the combined effects of the magnitude of the applied force, cycle rate and postural deviation would significantly impact quantitative measures of AF bulge in the IVD was rejected. Based on the results presented in this study, the magnitude of postural deviation was the only exposure variable that significantly affected the magnitude of IVD bulge.

Previously, Heuer et al. (2008) characterised the effect of posture on the AF bulge of the IVD after a 15 min preload with 500 N of static compressive force, which is similar to the loading protocol that was applied before the pre-test scans were captured in the present study. Results from this investigation revealed that the median IVD bulge was 1.90 mm (anterior) and –1.44 mm (posterior; inward bulge) when a 7.5 N m flexion moment was applied (Heuer et al., 2008). Interestingly, across all specimens that were included in the present study, the average (SD) pre-test AF bulge of the IVD measured at the midline of the anterior region of the IVD in a flexed posture was 1.35 (0.48) mm, which is less than what has been reported by Heuer et al. (2008). However, an important difference between our work is that the posterior structures remained intact in the present study, which Heuer et al. (2008) later showed that the median IVD bulge measured at the anterior region of the IVD in a flexed posture increased by approximately 1.4 × when the anterior longitudinal ligament and vertebral arches were removed (median bulge = 2.14 mm) compared to intact specimens (median bulge = 1.56 mm). These differences may also be attributable to the use of porcine cervical FSUs, which are approximately 50% of the size of human lumbar motion segments (Yingling et al., 1999), as well as the pre-conditioning loads that were applied to all specimens before testing.

The application of findings from this study to the *in vivo* human lumbar spine is limited by the use of porcine cervical FSUs, which does not take into account any physiological repair of the tissues or the natural restoration of intervertebral joint height in a healthy spine due to diurnal changes in fluid loss and reabsorption (Adams et al., 1987; Zander et al., 2010). It is also important to note that IVD height loss and AF bulging data are not meant to apply to clinical situations, particularly since the insertion of the anterior longitudinal ligament on the anterior face of the AF was removed to enable scanning of the AF. Previous research conducted by Heuer et al. (2008) has shown that the longitudinal ligaments stabilise the IVD and help prevent it from bulging. It should also be noted that due to regional differences in the mechanical and structural properties of the IVD, height loss and AF bulge measurements may not accurately depict the structural changes across all regions of the disc. However, our decision to use intact FSUs for testing precludes the ability image other regions of the AF. Lastly, it must be

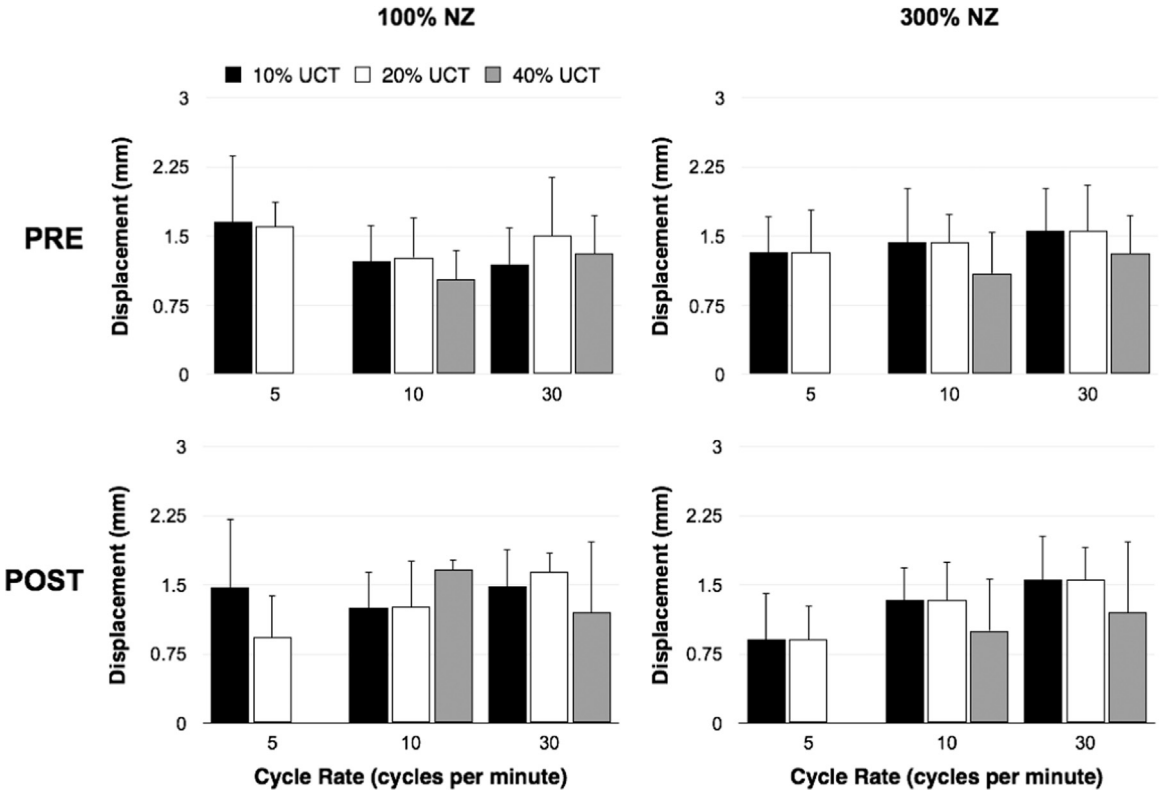

Fig. 7. Average pre- and post-test peak AF bulge of the intervertebral disc measured at the midline of the joint across experimental conditions. Specimens from the 5 cycles per minute, 100% neutral zone range, 40% UCT loading condition were excluded since there were no specimens that survived the entire loading protocol.

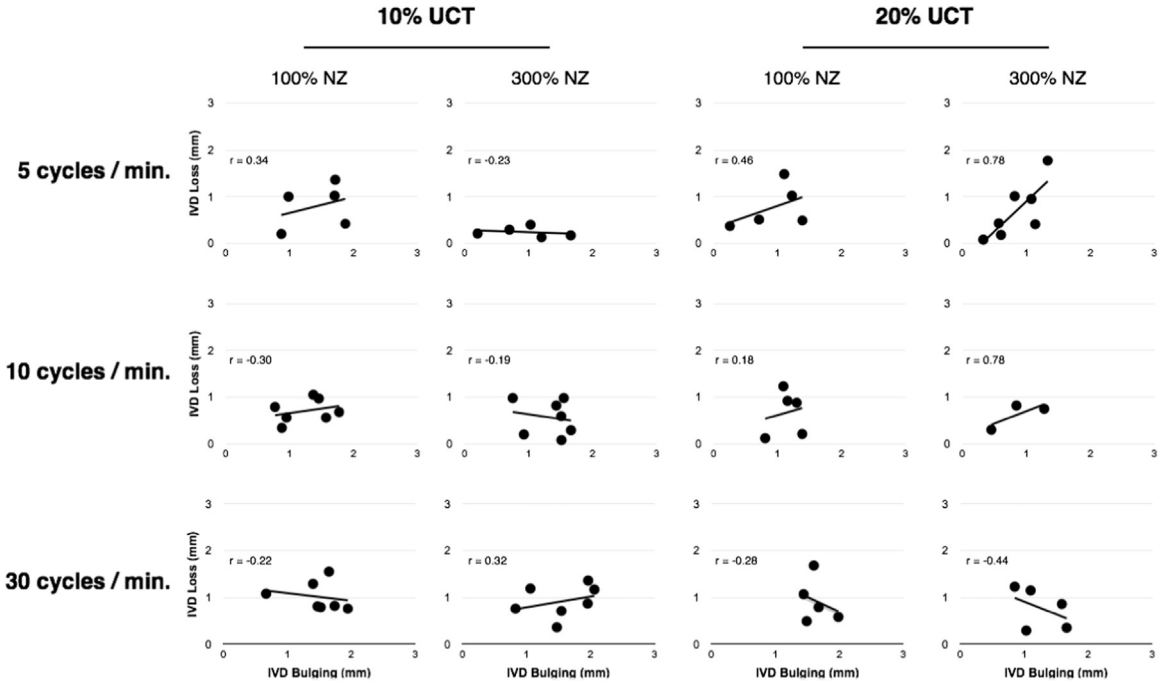

Fig. 8. Scatter plots illustrating linear regression analyses that were performed between intervertebral height loss and post-testing intervertebral disc bulging across experimental conditions in both the 10% and 20% ultimate compressive tolerance loading conditions.

acknowledged that the use of porcine cervical FSUs, which have a gelatinous nucleus pulposus, may have resulted in more pronounced AF bulging compared to aged human specimens.

In summary, this investigation provides basic science evidence that total specimen height loss is not an accurate depiction of IVD changes (as measured from the anterior surface of intact specimens) in all test scenarios. While interactions between force, posture and repetition impacted total specimen height loss, the IVD was not influenced by these interactions. The magnitude of the applied compressive load was the only independent factor that significantly impacted IVD height loss, as measured from the 3D surface profiles that were constructed from the laser scanner data.

Interestingly, postural deviation was the only exposure variable that significantly impacted the magnitude of peak AF bulge, pre/post-testing.

Conflict of interest statement

The authors have no conflicts to declare.

Acknowledgements

The authors would like to acknowledge funding provided by the Natural Sciences and Engineering Research Council of Canada (Grant No. 227638). JPC also holds the Canada Research Chair in Spine Biomechanics and Injury Prevention.

References

Adams, M.A., Dolan, P., Hutton, W.C., 1987. Diurnal variations in the stresses on the lumbar spine. Spine 12, 130–137.
Brinckmann, P., Biggemann, M., Hilweg, D., 1989. Prediction of the compressive strength of human lumbar vertebrae. Clin. Biomech. 4, 3–27.
Cohen, J., 1998. Statistical Power Analysis for the Behavioral Sciences: Second Edition. Lawrence Erlbaum Associates, Hillsdale, New Jersey.
Cuchanski, M., Cook, D., Whiting, D.M., Cheng, B.C., 2011. Measurement of occlusion of the spinal canal and intervertebral foramen by intervertebral disc bulge. Int. J. Spinal Surg. 5, 9–15.
Galante, J.O., 1967. Tensile properties of the human lumbar annulus fibrosus. Acta Orthop. Scand. Supplement. 100, 1–91.
Heuer, F., Schmidt, H., Wilke, H.J., 2008. The relation between intervertebral disc bulging and annular fiber associated strains for simple and complex loading. J. Biomech. 41, 1086–1094.
Oxland, T.R., Panjabi, M.M., Southern, E.P., Duranceau, J.S., 1991. An anatomic basis for spinal instability: a porcine trauma model. J. Orthop. Res. 9, 452–462.
Parkinson, R.J., Durkin, J.L., Callaghan, J.P., 2005. Estimating the compressive strength of the porcine cervical spine: an examination of the utility of DXA. Spine 30, E492–E498.
Parkinson, R.J., Callaghan, J.P., 2009. The role of dynamic flexion in spine injury is altered by increasing dynamic load magnitude. Clin. Biomech. 24, 148–154.
Stokes, I.A., 1988. Bulging of lumbar intervertebral discs: non-contacting measurements of anatomical specimens. J. Spinal Disord. 1, 189–193.
Thompson, R.E., Barker, T.M., Pearcy, M.J., 2003. Defining the neutral zone of sheep intervertebral joints during dynamic motions: an in vitro study. Clin. Biomech. 18, 89–98.
van der Veen, A.J., Mullender, M.G., Kingma, I., van Dieën, J.H., van, J.H., Smit, T.H., 2008. Contribution of vertebral bodies, endplates, and intervertebral discs to the compression creep of spinal motion segments. J. Biomech 41, 1260–1268.
Wenger, K.H., Schlegel, J.D., 1997. Annular bulge contours from an axial photogrammetric method. Clin. Biomech. 12, 438–444.
Yingling, V.R., Callaghan, J.P., McGill, S.M., 1999. The porcine cervical spine as a model of the human lumbar spine: an anatomical, geometric, and functional comparison. J. Spinal Disord. 12, 501–508.
Zander, T., Krishnakanth, P., Bergmann, G., Rohlmann, A., 2010. Diurnal variations in intervertebral disc height affect spine flexibility, intradiscal pressure and contact compressive forces in the facet joints. Comput. Methods Biomech. Biomed. Eng. 13, 551–557.